

## Research Article

# Risk Probabilistic Characteristics for Contaminated Porcelain Insulator in the Egyptian Sinai Desert

Mohammed El-Shahat <sup>1</sup>, Ibrahim Al-Naimi <sup>2</sup>, and Elsayed Tag-Eldin <sup>3</sup>

<sup>1</sup>Electrical Power Department, Faculty of Engineering, Cairo University, Giza, Egypt

<sup>2</sup>Electrical and Computer Engineering Department, College of Engineering, Sultan Qaboos University, Muscat, Oman

<sup>3</sup>Electrical Power Department, Faculty of Engineering, Future University, Cairo, Egypt

Correspondence should be addressed to Mohammed El-Shahat; [elbagalaty02010@gmail.com](mailto:elbagalaty02010@gmail.com)

Received 20 April 2023; Revised 14 June 2023; Accepted 23 June 2023; Published 3 July 2023

Academic Editor: Suman Lata Tripathi

Copyright © 2023 Mohammed El-Shahat et al. This is an open access article distributed under the Creative Commons Attribution License, which permits unrestricted use, distribution, and reproduction in any medium, provided the original work is properly cited.

Transmission lines in the desert are exposed to the desert environment, which includes sandstorms as one of its hallmarks. A conductive layer develops with prolonged sand deposition and the presence of moisture, ambient humidity, and dew. The ensuing leakage current causes surface discharge, which limits the life of the insulator and interrupting the power supply. The locations of power lines in the Egyptian Sinai desert, where sandstorms are known to occur frequently, are exposed to such a risk. In order to estimate the danger of insulator failure, this paper studies the flow of leakage current on porcelain insulators that have been contaminated with sand. This work relies on accurate data collected and published in a prior study regarding Sinai, which mainly focused on contaminating sand's grain sizes. Porcelain insulator is simulated using finite element method to determine the leakage current that results on its contaminated surface. The probabilistic characteristics of the insulator's leakage current are derived using Monte Carlo technique, allowing for the risk assessment of insulator failure. This assessment can be used to justify the suitability of using this kind of insulator in Sinai.

## 1. Introduction

Transmission lines in the desert area are subject to harsh environmental conditions, including sandstorms. During sandstorms, the sand particles can also accumulate on the insulators and other components of the transmission lines, leading to reduced performance and increased risk of failure [1–4]. When an insulator's surface becomes contaminated with pollutants such as dust, salt, or other conductive materials, it can create a conductive path for electrical current to flow through. This can lead to a leakage current, which can cause heating and deterioration of the insulator's surface [5–7]. Over time, this can weaken the insulation and increase the risk of a power outage or even a catastrophic failure of the power line. To prevent leakage current on insulators surfaces, regular maintenance and cleaning are necessary such as water washing, mechanical brushing, or abrasive blasting. Ultimately, the cost of insulator cleaning

must be weighed against the potential costs of a power outage or insulation failure, which can be much more significant. The level of contamination and salinity, which in turn influences the conductivity of the contamination layer, determines the amount of the leakage current on a polluted insulator surface [8–12]. Porcelain insulators are commonly used in high voltage power lines due to their excellent electrical and mechanical properties. However, the surface of porcelain insulators becomes contaminated with pollutants and affects their performance [13, 14]. In desert atmospheric weather, the thickness of the pollution layer that built up on the insulator surface is dependent on the type of soil present in the area as well as the size of the contaminating sand grains [15]. The leakage current would flow on the insulator's surface when sand is deposited and there is a significant source of wetting, such as dew in the morning. This current can cause heating of the conductive sand layer, which in turn can lead to the formation of dry bands. These dry bands can

then result in surface flashover, which can damage the insulator and cause power outages. It is therefore important to monitor the contamination level on insulators to prevent such occurrences [16–20].

It is clear that there have been several previous studies conducted to investigate the effects of pollution on insulators. These studies have employed various analytical and experimental methods to estimate parameters such as current density distribution, flashover, and leakage current under different conditions. For example, a study estimated the risk and performance of composite insulator in Sinai desert [15, 21], while another study computed the current density distribution and flashover along the polluted insulator surface in desert pollution [1, 22]. Another one considered the amount of salt in the contaminated layer when simulating the leakage current [4, 23]. In addition, numerical and experimental investigations were used in some studies to calculate the flashover on porcelain polluted insulators and estimate the dielectric strength [2, 24]. Other investigations have used statistical methods to assess the risk of leakage current caused by various contamination layers along insulators such as glass or silicone rubber [3, 10]. These studies are important in understanding the behavior of insulators under different pollution levels and designing appropriate measures to maintain their performance [25].

This research focuses on the primary cause of insulator failure under power-frequency voltage, which is leakage current on surface pollutants. The 3D COMSOL software program, which is based on the finite element approach, is used to simulate insulators. A conventional two-shed porcelain insulator that could be utilized on 220 kV power lines is used as a simulated case study. These leakage current distributions are computed with various sand conductivities and sand grain thicknesses using actual data from a previous study based on sand samples gathered from the Sinai desert near the transmission line [9]. In that investigation, the salinity and subsequent conductivity of random samples of soil from the desert are used to determine the statistical distributions of the size of the sand grains. The overall probability density distribution of leakage current is derived using statistical distribution mapping based on the estimated effects of sand grain size and salinity on the resulting leakage current. Finally, the risk of insulator failure is calculated using the cumulative statistical distribution of leakage current. This research provides valuable insights into the factors that contribute to insulator failure under power-frequency voltage and can help in developing strategies to prevent such failures.

## 2. Methods

This research uses a 220 kV porcelain long rod insulator with technical specifications data according to IEC 60274 and IEC 60383. These specifications define the requirements for insulators used in high voltage power systems. The dimensions of this insulator are provided in Table 1, and the insulator is shown in Figure 1(a). The dimensions of the insulator are important factors in determining its electrical performance and its ability to withstand the environmental factors. The

TABLE 1: Porcelain insulator specifications and dimensions.

System voltage (kV)	220
Type of string	Single tension
Length of insulator (mm)	2550
Creepage distance (mm)	5550
No. of insulator units per string	1 * 2
Tensile strength (kN)	160
Core diameter (mm)	75
No. of discs	15
Size of the disc (mm)	305 * 170

use of standardized specifications and testing procedures helps ensure that insulators used in power systems meet minimum performance requirements and are safe and reliable.

The insulator model was built using the finite element method software by defining the material of porcelain. Since analyzing the distribution of leakage current along the entire insulator is a time-consuming procedure that is unnecessary, a sector consisting of two sheds with a creepage distance of 355.3 mm is selected to simulate the leakage current. The boundary conditions, including local potential and electric field, resulting from those conditions were set around this sample sector of the insulator. A suitable finite element meshes were employed to the sector of insulator as shown in Figure 1(b). The tangential (surface) current is then produced from the directional components of the leakage current density as a result from the software. This step analyzes the distribution of leakage current in the selected sector of the insulator.

## 3. Results and Discussion

The boundary conditions are applied to the chosen sample insulator simulation section, where the potentials at the sample sector's two ends, as determined by the global analysis. The values of the potentials at the ends of the sample are 53.142 kV and 48.952 kV. The potential distribution is influenced by several factors, including the insulator's shape, surface condition, and the electric field in the surrounding environment. The distribution may be non-linear due to many factors such as the surface leakage current, corona discharge, tracking, and erosion [26]. This work assumes a linear potential distribution in clean and contaminated cases. Sand grains with diameters between 1 and 2 mm, which predominate in Sinai according to statistical distributions of sand particle sizes published in a previous study [15], are selected. This range of grain sizes is used in the research, and it is assumed that sufficient accumulation will result in an equal-thickness contaminated layer. Thus, the contaminated layer along the entire insulator has a thickness ranging from 1 mm to 2 mm. In addition, a chemical analysis of the collected samples indicated the pollution layer's equivalent salt content (ESC, measured in mg of salt per g of sand). It was found that the most likely salinity range to be found in Sinai was between 0.5 and 1.5 mg salt/g sand [15].

The solution salinity is first derived from the below expression in order to transform the salt content expressed

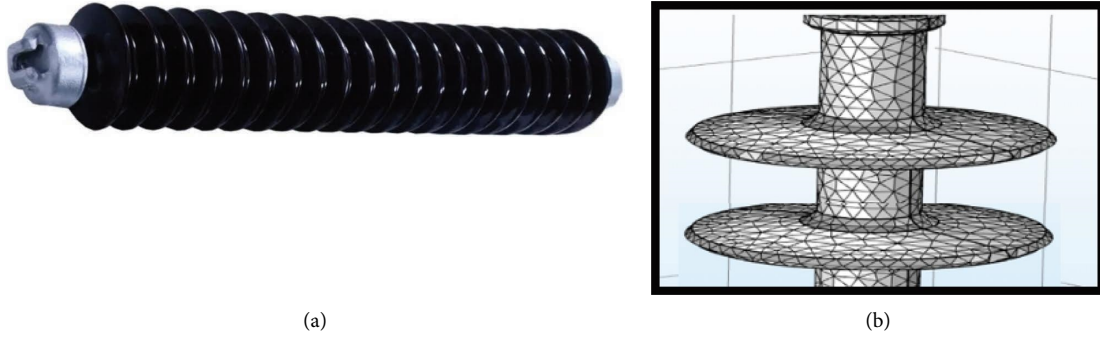


FIGURE 1: Porcelain long rod insulator: (a) complete unit and (b) simulated sample sector.

in ESC (mg of salt/g of sand), as provided by the chemical analysis, into pollution layer electrical conductivity ( $\mu\text{S/m}$ ) [9, 17].

$$S_a = \text{ESC} * W, \quad (1)$$

where  $S_a$  is the salinity of the solution and  $W$  is the quantity of sand (mg) that is placed on insulator's surface with a specific volume of water. Salinity of the layer is then linked to the solution's electrical conductivity as follows [4]:

$$S_a = (5.7 * \sigma_{20})^{1.03}, \quad (2)$$

where  $\sigma_{20}$  is the conductivity ( $\mu\text{S/m}$ ) at a temperature of  $20^\circ\text{C}$ . The quantity  $W$  can be written out using the lattice geometry theories as follows:

$$W = \frac{\lambda * \rho}{1 - \lambda}, \quad (3)$$

where  $\lambda$  is the lattice arrangement density, which is the measure of how much sand actually occupy a certain region, and  $\rho$  is the specific gravity of wet sand (1.92 g/ml) [15]. According to calculations, the parameter  $\lambda$  can be within the range from 0.523 to 0.740 depending on how compact the system [17]. This work uses lattice arrangement density of 0.523 as a worst-case study to get higher quantity of sand on insulators.

To get the necessary electrical conductivity, the aforementioned relations are applied over the ESC's specified operating range. With the value  $W = 2.1$  g/ml, Table 2 displays the various conductivities of sand grains taken from the Sinai desert according to their ESC range. In order to find the statistics of the leakage current, the values shown in Table 2 are considered in polluted insulator simulation. The impact of those conductivities in each contaminated layer of the leakage current on the insulator surface is simulated.

The distribution of leakage current along the sector of insulator creepage distance is shown in Figure 2 for 1 mm thickness of contamination layer with conductivity of  $284.9 \mu\text{S/cm}$ . The surface leakage current is calculated by the surface integration of the current densities, and it is 65.5 mA.

Figure 3 shows the impacts of various conductivities on the current density distribution on insulator creepage distance at 2 mm thickness of contaminated layer. Also, Figure 4 shows the impact of different contamination layer

TABLE 2: Conductivity estimation from ESC and salinity.

ESC (mg salt per g sand)	$S_a$ (mg/ml)	$\sigma_{20}$ ( $\mu\text{S/cm}$ )
0.5	1.05	284.9
1.0	2.10	558.4
1.5	3.15	827.8

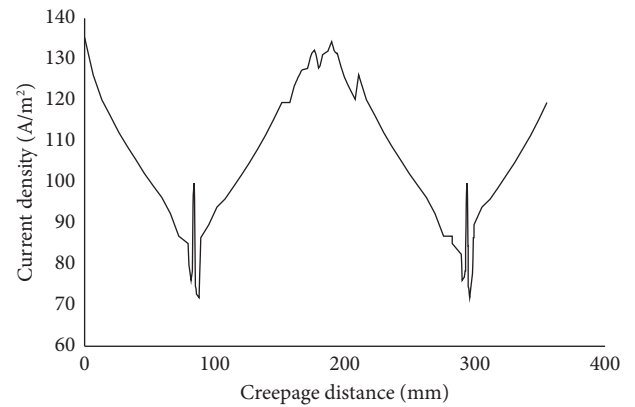


FIGURE 2: Current density distribution for 1 mm contaminated layer with conductivity  $284.9 \mu\text{S/cm}$ .

thickness on the current density distribution at conductivity  $284.9 \mu\text{S/cm}$ . All the results for surface leakage current are summarized in Table 3 for different cases of conductivities and contamination layer thicknesses.

**3.1. Dependence of Leakage Current on Sand Grain Size and Conductivity.** Numerical derivation is involved to find the relationship between leakage current with contamination layer conductivity and sand grain sizes. The relationship between leakage current and conductivity with different grain sizes is shown in Figure 5. In addition, the relationship between leakage current and grain size at different conductivities is shown in Figure 6. The interdependence of the leakage current on contamination conductivity and the thickness of grain size on insulator surface are used to derive the statistics of leakage current, which become the basis for the insulator failure risk assessment. This joint dependence of leakage current is derived numerically and the characteristics are depicted in Figure 7. According to these

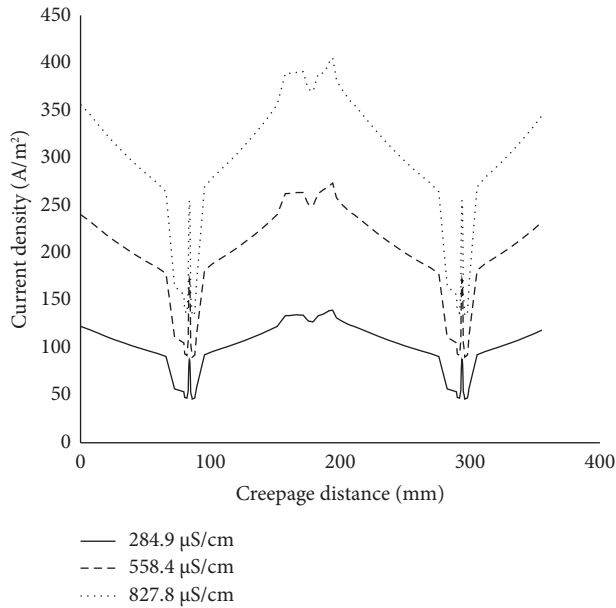


FIGURE 3: Current density distribution with various conductivities at contaminated layer thickness 1 mm.

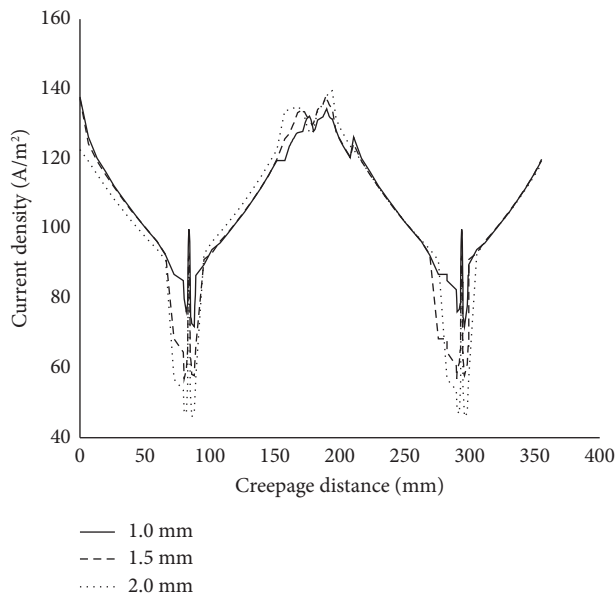


FIGURE 4: Current density distribution with different contamination layer thickness at conductivity 284.9 (μS/cm).

TABLE 3: Leakage current (mA) for different layer thickness and conductivity.

Layer thicknesses	Conductivity		
	284.9 (μS/cm)	558.9 (μS/cm)	827.8 (μS/cm)
1.0 (mm)	76.44	134.4	197.22
1.5 (mm)	78.72	137.68	204.1
2.0 (mm)	82.5	161.7	239.71

analyses, the results indicate that changing the conductivity has a significant effect on the leakage current, while the effect of grain size is relatively small.

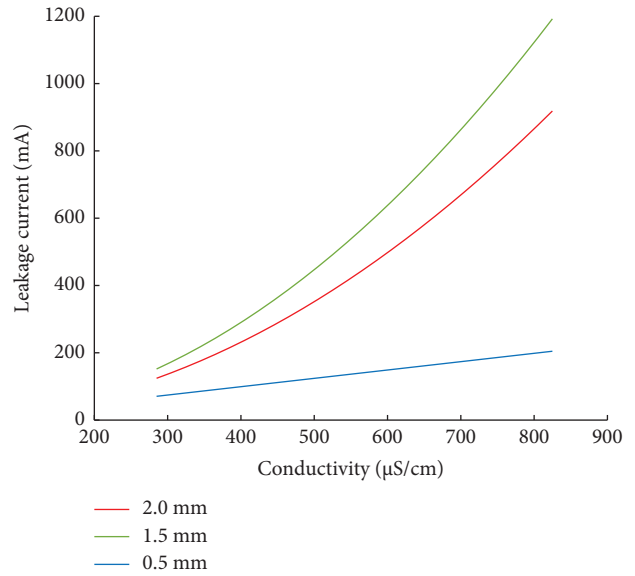


FIGURE 5: Relation between leakage current with conductivity at different grain size.

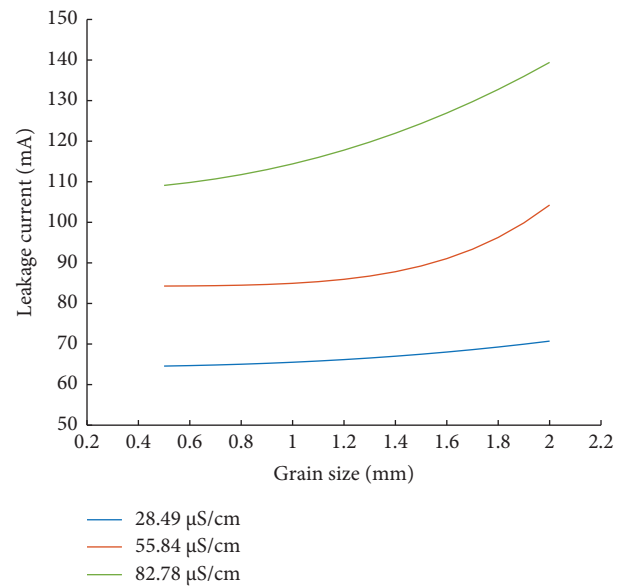


FIGURE 6: Relation between leakage current with grain size at different conductivities.

3.2. Probability Density Function of Leakage Current. The statistical analysis of the leakage current in terms of two variables: contamination layer thickness and its conductivity is derived depending on the abovementioned data. These variables are treated as random variables, which mean they can be described statistically. The leakage current can also be considered a random variable, with its probability density distribution being a combination of the conductivity and thickness of the contamination layer. The paper also assumes that the random variables  $x$  (conductivity) and  $y$  (grain size) are independent. This means that the probability density function of the random variable  $z$  (leakage current) can be calculated as the product of the probability density functions of  $x$  and  $y$ , i.e.,  $P(z) = P(x) * P(y)$ .

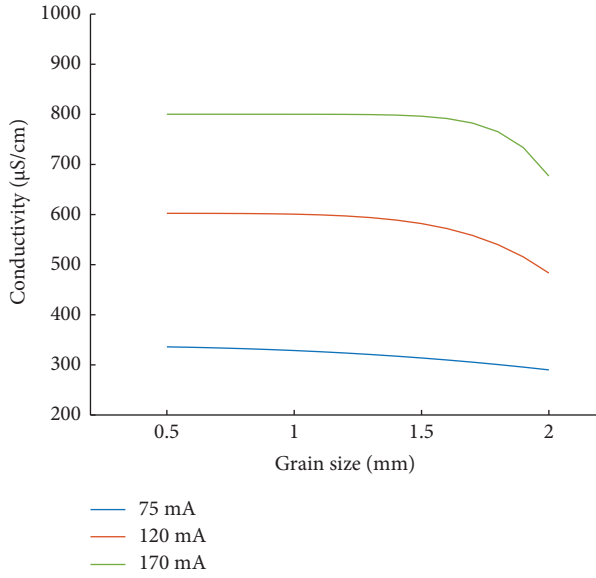


FIGURE 7: Interdependence of leakage current on conductivity and grain size.

Depending on the samples collected of sands in Sinai [9], the frequency distribution of ESC was calculated and then the probability density function  $P(x)$  was derived. It was found that  $P(x)$  is represented as Beta distribution; its average is  $298.7 \mu\text{S}/\text{cm}$ , and standard deviation is  $557.4 \mu\text{S}/\text{cm}$  [9]. Also, the frequency distribution of grain size was calculated and then the probability density function  $P(y)$  was derived. It was found that  $P(y)$  is represented as lognormal distribution; its average is  $0.401 \text{ mm}$ , and standard deviation is  $0.346 \text{ mm}$  [15].

The Monte Carlo technique is used to derive the probability density function of leakage current,  $P(z)$ , based on the data mentioned earlier. The Monte Carlo technique is a mathematical simulation technique that is often used to incorporate risk into quantitative analysis [15]. The Monte Carlo simulation involves creating models of potential outcomes and replacing each factor that has intrinsic uncertainty with a range of values, represented by a probability distribution. Then, the simulation repeatedly calculates the outcomes using a new set of random values drawn from the probability distributions. Depending on the number of uncertainties and the ranges assigned to them, the Monte Carlo simulation may require thousands or tens of thousands of recalculations. The probability function of leakage current is calculated by repeatedly generating new sets of random values of the variables (i.e., conductivity and the grain size). The procedure for carrying out these calculations is described in detail in reference [15]. The overall probability of leakage current is formed using a sufficiently large sample of calculated values, which are displayed in Figure 8. It is found that the best distribution to represent the leakage current is Weibull distribution. The probability density function is expressed as follows:

$$P(z, \lambda, k) = \frac{k}{\lambda} \left(\frac{z}{\lambda}\right)^{k-1} e^{-(z/\lambda)^k}. \quad (4)$$

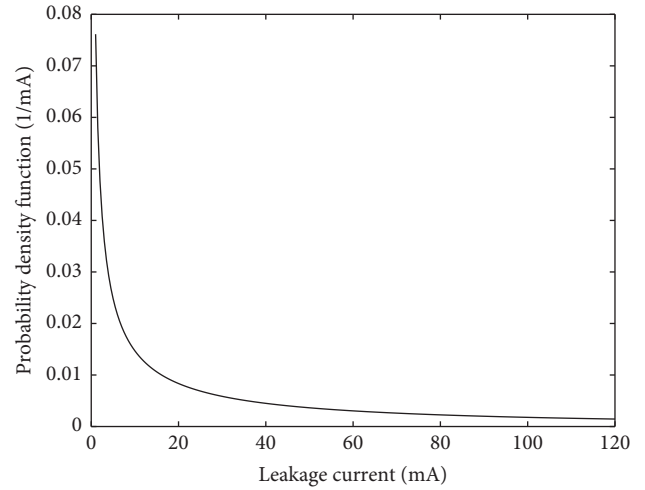


FIGURE 8: Probability density function of the leakage current.

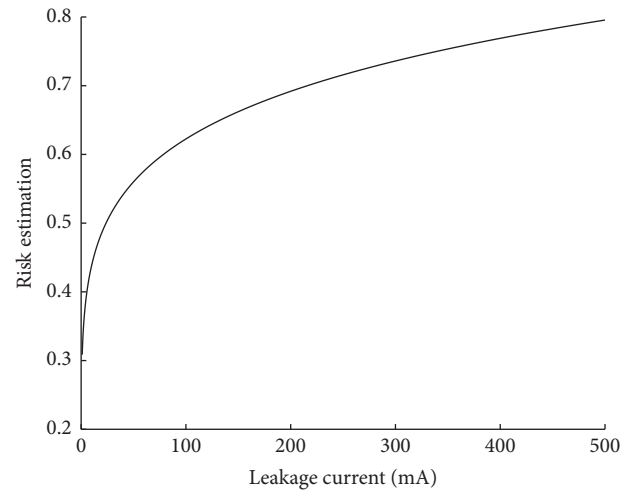


FIGURE 9: Risk estimation of porcelain insulator failure.

The statistical parameters in (4) are  $\lambda = 41.4$  and  $k = 0.52$ . The mean value of leakage current is  $81 \text{ mA}$ , and the standard deviation is  $22 \text{ mA}$  with a square error of  $0.02348$ . The average value represents the expected value of the leakage current based on the given statistical parameters. It is worth noting that these statistics data will vary for different cases, as they depend on the specific conditions and variables that are involved in each case. Therefore, the statistical analysis should be carried out for each specific case separately, in order to obtain accurate and relevant results.

**3.3. Risk Failure Assessment.** The probability distribution of leakage current can be used to evaluate the chance of insulator failure. The cumulative probability of the leakage current can be generated using the probability density distribution. This cumulative probability function shows the maximum limits of the leakage current that should not be exceeded for certain risk value and thus indicates the probability of insulator failure. The resulting cumulative probability function can be displayed graphically, as shown

in Figure 9. The figure shows the danger of insulator failure in conditions of desert pollution for a specific insulator located in the currently stated environment and operating at a 220 kV power line. The critical leakage current value of 200 mA is used as an example to illustrate the risk of insulator failure. According to Figure 9, this critical leakage current value indicates a 68% probability of insulator failure.

In summary, the probability distribution of leakage current provides a useful tool for evaluating the risk of insulator failure under different conditions. The resulting cumulative probability function shows the probability of exceeding a given leakage current value and can be used to inform decisions and actions related to insulator maintenance and replacement.

#### 4. Conclusion

This work describes the process of simulating the leakage current density on porcelain insulator under various conditions of desert pollution using the finite element method. The simulation considers different contaminated layer thickness and salinity (conductivity) levels. The result of the simulation is the total magnitude of leakage current on a porcelain insulator sector under the given conditions.

Based on the simulation results, the relation between leakage current, conductivity, and grain size is estimated numerically. The leakage current is expressed statistically as a bivariate random variable with conductivity and grain size as independent variables. The Monte Carlo technique is used to derive the probability density function of leakage current from this bivariate distribution.

The resulting probability density function is fitted to a lognormal distribution with a mean leakage current value of 81 mA. This statistical distribution provides an accurate representation of the leakage current distribution under the given conditions. The cumulative probability function of the leakage current is used in this study as a direct tool for assessing the risk of insulation failure. This function shows the probability that a given leakage current value will be exceeded, and thus, it indicates the risk of insulator failure.

In the future work, it is required to study the performance of different types of electrical insulator (silicone rubber and glass) at higher voltage system of 500 kV. This is also existed in Sinai desert and is affected by the same contamination conditions.

#### Data Availability

The data used to support the study are available from the corresponding author upon request.

#### Conflicts of Interest

The authors declare that they have no conflicts of interest.

#### Acknowledgments

This research was fully funded by Future University, Egypt.

#### References

- [1] E. Al-Mahdawi, "Experimental study of porcelain and toughened glass suspension insulators under desert contamination," *IOP Conference Series: Earth and Environmental Science*, vol. 779, no. 1, Article ID 12060, 2021.
- [2] A. A. Salem, R. Abd-Rahman, W. Rahiman et al., "Pollution flashover under different contamination profiles on high voltage insulator: numerical and experiment investigation," *IEEE Access*, IEEE, vol. 9, pp. 37800–37812, 2021.
- [3] A. A. Salem, R. Abd-Rahman, S. A. Al-Gailani et al., "Risk assessment of polluted glass insulator using leakage current index under different operating conditions," *IEEE Access*, IEEE, vol. 8, pp. 175827–175866, 2020.
- [4] S. Mohammadnabi and K. H. Rahmani, "Influence of humidity and contamination on the leakage current of 230-kV composite insulator," *Electric Power Systems Research*, Elsevier, vol. 194, 2021.
- [5] A. A. Salem, K. Y. Lau, M. T. Ishak et al., "Monitoring porcelain insulator condition based on leakage current characteristics," *Materials*, vol. 15, no. 18, p. 6370, 2022.
- [6] A. A. Salem, K. Y. Lau, Z. Abdul-Malek et al., "Polymeric insulator conditions estimation by using leakage current characteristics based on simulation and experimental investigation," *Polymers*, vol. 14, no. 4, p. 737, 2022.
- [7] L. Maraaba, K. Al-Soufi, T. Ssennoga, A. M. Memon, M. Y. Worku, and L. M. Alhems, "Contamination level monitoring techniques for high-voltage insulators: a review," *Energies*, vol. 15, no. 20, p. 7656, 2022.
- [8] A. A. Salem, K. Y. Lau, W. Rahiman et al., "Leakage current characteristics in estimating insulator reliability: experimental investigation and analysis," *Scientific Reports*, vol. 12, no. 1, Article ID 14974, 2022.
- [9] B. Cao, Y. Liu, Z. Li, S. Shen, L. Wang, and Z. Wang, "Assessment of insulator pollution degree based on contamination moisture with temperature change," *IEEE Sensors Journal*, vol. 22, no. 21, pp. 21172–21178, Oct. 2022.
- [10] N. F. Sopelsa Neto, S. F. Stefenon, L. H. Meyer, R. G. Ovejero, and V. R. Leithardt, "Fault prediction based on leakage current in contaminated insulators using enhanced time series forecasting models," *Sensors*, vol. 22, no. 16, p. 6121, 2022.
- [11] D. Maadjoudj, A. Mekhalidi, and M. Tegar, "Flashover process and leakage current characteristics of insulator model under desert pollution," *IEEE Transactions on Dielectrics and Electrical Insulation*, IEEE, vol. 25, no. 6, pp. 2296–2304, 2018.
- [12] H. Rosli, N. A. Othman, N. A. Jamail, and M. N. Ismail, "Potential and electric field characteristics of broken porcelain insulator," *International Journal of Electrical and Computer Engineering*, vol. 7, no. 6, p. 3114, 2017.
- [13] A. P. Mishra, R. S. Gorur, and S. Venkataraman, "Evaluation of porcelain and toughened glass suspension insulators removed from service," *IEEE Transactions on Dielectrics and Electrical Insulation*, IEEE, vol. 15, no. 2, pp. 467–475, 2008.
- [14] O. E. Gouda and A. Z. El Dein, "Simulation of overhead transmission line insulators under desert environments," *IET Generation, Transmission and Distribution*, vol. 7, no. 1, pp. 9–13, 2013.
- [15] M. El-Shahat and H. Anis, "Risk assessment of desert pollution on composite high voltage insulators," *Journal of Advanced Research*, Elsevier, vol. 5, no. 5, pp. 569–576, 2014.
- [16] A. El-Hag, S. Jayaram, and E. Cherney, "Calculation of current density along insulator surface using field and circuit theory approaches," in *Proceedings of the Annual Report Conference*

- on *Electrical Insulation and Dielectric Phenomena*, October, 2003.
- [17] H. Cohn and A. Kumar, "The densest lattice in twenty-four dimensions," *Electronic Research Announcements of the American Mathematical Society*, vol. 10, no. 7, pp. 58–67, 2004.
- [18] M. El-Shahat and H. Anis, "Assessing partial discharge on composite insulators under desert pollution conditions," *International Journal of Emerging Technology and Advanced Engineering*, vol. 3, no. 7, 2013.
- [19] A. A. Salem, R. Abd-Rahman, S. A. Al-Gailani, M. S. Kamarudin, H. Ahmad, and Z. Salam, "The leakage current components as a diagnostic tool to estimate contamination level on high voltage insulators," *IEEE Access*, vol. 8, pp. 1–92528, 2020.
- [20] M. Asadpoor, "Simulation and measurement of the voltage distribution on high voltage suspension porcelain insulator string under pollution condition," *International Journal of Applied Science and Engineering Research*, vol. 1, no. 1, pp. 165–175, 2012.
- [21] I. Ahmadi-Joneidi, A. A. Shayegani-Akmal, and H. Mohseni, "Leakage current analysis of polymeric insulators under uniform and non-uniform pollution conditions," *IET Generation, Transmission and Distribution*, vol. 11, no. 11, pp. 2947–2957, 2017.
- [22] K. Naito, Y. Mizuno, and W. A. Naganawa, "A study on probabilistic assessment of contamination flashover of high voltage insulator," *IEEE Transactions on Power Delivery*, vol. 10, no. 3, pp. 1378–1384, 1995.
- [23] R. Shariatinasab, S. Saghafi, M. Khorashadizadeh, and M. Ghayedi, "Probabilistic assessment of insulator failure under contaminated conditions," *IET Science, Measurement and Technology*, vol. 14, no. 5, pp. 557–563, 2020.
- [24] M. M. Hussain, S. Farokhi, S. G. McMeekin, and M. Farzaneh, "Risk assessment of failure of outdoor high voltage polluted insulators under combined stresses near shoreline," *Energies*, vol. 10, no. 10, p. 1661, 2017.
- [25] A. Cavallini, G. C. Montanari, and F. Ciani, "Analysis of partial discharge phenomena in paper-oil insulation systems as a basis for risk assessment evaluation," in *Proceedings of the IEEE International Conference on Dielectric Liquids (ICDL)*, pp. 241–244, Coimbra, Portugal, June, 2005.
- [26] B. Zhang, Y. Cui, W. Zhang et al., "Voltage and electric field distribution along porcelain long rod insulator string in AC 500kV transmission line," in *Proceedings of the IEEE International Conference on High Voltage Engineering and Application (ICHVE)*, pp. 1–4, Chengdu, China, September, 2016.